Smart Structures and Systems, *Vol. 24, No. 2 (2019) 173-182*
DOI: https://doi.org/10.12989/sss.2019.24.2.173

Impact location on a stiffened composite panel using improved linear array

Yongteng Zhong[a] and Jiawei Xiang[*]

College of Mechanical and Electrical Engineering, Wenzhou University, Wenzhou, 325035, P.R. China

(Received October 23, 2018, Revised April 13, 2019, Accepted April 26, 2019)

Abstract. Due to the degradation of beamforming properties at angles close to 0° to 180°, linear array does not have a complete 180° inspection range but a smaller one. This paper develops a improved sensor array with two additional sensors above and below the linear sensor array, and presents time difference and two dimensional multiple signal classification (2D-MUSIC) based impact localization for omni-directional localization on composite structures. Firstly, the arrival times of impact signal observed by two additional sensors are determined using the wavelet transform and compared, and the direction range of impact source can be decided in general, 0°to 180° or 180° to 360°. And then, 2D-MUSIC based spatial spectrum formula using uniform linear array is applied for locate accurate position of impact source. When the arrival time of impact signal observed by two additional sensors is equal, the direction of impact source can be located at 0°or 180° by comparing the first and last sensor of linear array. And then the distance is estimated by time difference algorithm. To verify the proposed approach, it is applied to a quasi-isotropic epoxy laminate plate and a stiffened composite panel. The results are in good agreement with the actual impact occurring position.

Keywords: improved linear array; omni-directional; impact localization; 2D-MUSIC; time difference

1. Introduction

Structural health monitoring is an important requirement for detecting, estimating, classifying, and predicting damage in engineering structures (Yuan *et al.* 2005, Cheng *et al.* 2014). Composite materials have a number of potential advantages over conventional materials since they can be designed to increase performance in a number of applications including specific stiffness, specific strength. However, these components are sensitive to low-velocity impact damages which can considerably degrade the structural integrity. Therefore, impact monitoring is an important research for structural health monitoring (Chang *et al.* 2017, Mahzan *et al*. 2010, Qiu *et al.* 2011).

Several methods using compact sensor array arrangement have been reported for structural health monitoring. Linear arrays, as the simplest and most widely used ones, have been well explored and developed. Pureka *et al*. (2010) described a damage detection technique on isotropic plates based on the properties of a linear phased array with piezoelectric sensors. Phased arrays also can be used as directional filters for damage detection application in structures. Purekar and Pine (2004) presented research on phased array filters using linear array to actively interrogate the orthotropic composite plate. Wang *et al*. (2011) proposed a spatial filter based damage imaging method improved by complex Shannon wavelet transform for an aircraft composite oil tank. Lee *et al.* (2011) presents the method of identifying the location of the multiple impacts on a plate using the time-frequency analysis and the kalman filter which well be applied to the real-time heath monitoring of the steam generator.

Among them, an array signal processing technology called Multiple Signal Classification (MUSIC) was developed for impact monitoring of plate-like structures. MUSIC algorithm shows better performance in comparison with single-molecule localization techniques (Agarwal *et al.* 2016). Chen (2010) develops the MUSIC-type method to the detection of point-like scatterers and uses the finite element method to simultaneously obtain the back ground Green's function at all points. Yang *et al*. (2013) employ MUSIC algorithm to estimate the direction of arrival (DOA) of one impact on an aluminum plate. Lee *et al.* (2014) proposed a new method for impact source localization in a plate based on the MUSCI and wavelet analysis. The authors in previous work propose the 2D-MUSIC algorithm based impact localization method for composite plate using the uniform linear array (Zhong *et al.* 2014, Yuan *et al.* 2014). Yuan *et al.* (2015) proposes a single frequency component-based re-estimated MUSIC algorithm to reduce the localization error caused by the anisotropy of the complex composite structure. Linear arrays have been proved that it can successfully detect the damage or locate impact source by performing area scanning and imaging with Lamb waves.

However, the linear array does not have a complete 180° inspection range but a smaller one due to the degradation of beamforming properties at angles close to 0° to 180°. The generally way to overcome the shortcomings of linear arrays is to adopt a two dimensional (2-D) array design

*Corresponding author, Professor
E-mail: wxw8627@163.com
[a] Ph.D.

ISSN: 1738-1584 (Print), 1738-1991 (Online)

configuration. Wang *et al.* (2015) propose an ultrasonic phased array based omni-directional damage detection and localization with a cruciform piezoelectric. Ren *et al.* (2017) develop a scanning spatial-wavenumber filter approach for multi-impact location in aircraft composite structures using cross-shaped array. Engholm and Stepinski (2011) present MUSIC algorithm based method to estimate the DOA on an aluminum plate using a uniform circular array. In our previous work, a novel 2D-MUSIC method is proposed for velocity self-estimated and for omni-directional impact localization in composite structures using plum-blossom sensor array (Zhong *et al.* 2016). Giurgiutiu (2001) performs simulation of the beamforming patterns of several 2-D sensor arrays, including cross shaped, rectangular fence, circular ring, rectangular grid, circular grid. His studies results show that the choice for implementation of these array types depends on the specialist's preferences and available manufacturing facilities. However, since the complex structures leaves narrow space for array arrangement due to the existing bolt holes, stiffeners, etc., and bolt holes and stiffeners will reduce the transmission and reception consistency of each sensor element in 2-D sensor arrays. Obviously, array types which have fewer elements and is arranged more compact are more suitable for complex structures.

As we know, linear array suffers from the half-plane mirror effect when it cover from 0° to 360°, which does not allow discriminating between a target placed above the array and a target placed below the array. Aim at its inherent characteristic, an improved linear array with two additional sensors above and below the linear sensor array is designed, and this paper develops time difference and 2D-MUSIC based impact localization for full range 360° impact localization on complex composite structures. Firstly, the arrival times of impact signal observed by two additional sensors are determined using the wavelet transform and compared, and the direction range of impact source can be decided in general, 0°to 180° or 180° to 360°. And then, 2D-MUSIC based spatial spectrum formula using uniform linear array is applied for locate accurate position of impact source. When the arrival time of impact signal observed by two additional sensors is equal, the direction of impact source can be located at 0°or 180° by comparing the first and last sensor of linear array. And then the distance is estimated using time difference algorithm.

The layout of the paper is as follows: Section 2 presents omni-directional impact location using an improved linear array. In section 3, Impact monitoring experiment is preformed on quasi-isotropic epoxy laminate plate. And omni-directional impact location using an improved linear array is preformed a large stiffened composite structure in section 4 to verify the proposed method.

2. Omni-directional impact location using an improved linear array

Consider the improved linear array depicted in Fig. 1. The array includes a uniform linear array which consist of 2M+1 piezoelectric (referred as PZT in the rest of this paper) sensors, i = -M, -M+1, …0, …, M-1, M, spaced at equal distance d, and two additional elements above and below the array labeled as PZT U and PZT D.

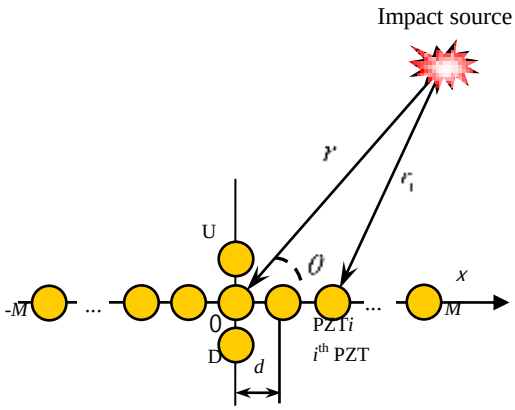

Fig. 1 Schematic of an improved uniform linear array

2.1 2D-MUSIC based impact localization method using uniform linear array

Assume a target located at impact source. The target position is at an elevation polar coordinate as measured. Seen as Fig. 1, θ denotes the wave propagating direction with respect to the horizontal axis, r is defined as the distance between the impact source and origin of the polar coordinates, and r_i is defined as the distance between the impact source and i^{th} PZT.

In the authors' previous study, 2D-MUSIC method for impact localization using uniform linear array is derived in detail (Yuan *et al.* 2014). Based on the previous study, the observed signal vector of the linear array can be represented as

$$\boldsymbol{X}(t) = \boldsymbol{A}(r,\theta)\boldsymbol{s}(t) + \boldsymbol{N}(t) \tag{1}$$

where

$$\mathbf{X}(t) = [\mathbf{x}_{-M}(t), \cdots, \mathbf{x}_i(t), \cdots, \mathbf{x}_M(t)]^{\mathrm{T}}$$

$$\mathbf{A}(r,\theta) = [a_{-M}(r,\theta), \cdots, a_i(r,\theta), \cdots, a_M(r,\theta)]^{\mathrm{T}}$$

$$\mathbf{N}(t) = [\mathbf{n}_{-M}(t), \cdots, \mathbf{n}_i(t), \cdots, \mathbf{n}_M(t)]^{\mathrm{T}}$$

and $\mathbf{s}(t)$ is the narrow-band signal with a central frequency ω_0 of impact source signal. Since the original impact signal is wide-band, the Gabor wavelet transform is used to extract the narrow band signals from the sensor outputs (Qiu and Yuan *et al.* 2009). $\mathbf{x}_i(t)$ denotes the output from PZT i of the sensor array observed at time t, $\mathbf{n}_i(t)$ is the output corresponding to the background noise.

The array steering vector $a_i(r,\theta)$ for the impact signal can be represented using complex signal as

$$a_i(r,\theta) = \frac{r}{r_i}\exp(j\omega_0\tau_i) \tag{2}$$

where the arriving time difference τ_i between PZT i and PZT 0 is represented by its second-order Taylor expansion as

$$\tau_i = \frac{(-d\cos\theta)}{c}(i-1) + (-\frac{d^2}{cr}\sin^2\theta)(i-1)^2 \quad (3)$$

Finally, 2D-MUSIC spatial spectrum can be calculated for impact localization using linear array is

$$\mathbf{P}(r,\theta) = \frac{1}{\mathbf{A}^{\mathrm{H}}(r,\theta)\mathbf{U}_{\mathrm{N}}\mathbf{U}_{\mathrm{N}}{}^{\mathrm{H}}\mathbf{A}(r,\theta)} \quad (4)$$

where $\mathbf{U}_{\mathrm{N}}$ denotes the noise subspace spanned by the eigenvector matrix corresponding to those small eigenvalues and estimated with eigenvalue decomposition of the covariance matrix $\hat{R}$, and the covariance matrix $\hat{R}$ can be calculated by

$$\hat{R} = \frac{1}{N}\mathbf{X}\mathbf{X}^{\mathrm{H}} \quad (5)$$

By varying r and θ as virtually scanning, $\mathbf{P}(r,\theta)$ of the whole monitored area could be obtained. The peak point on the spatial spectrum corresponds to the impact source point. Both the distance and direction of the source can be obtained as

$$(\hat{r},\hat{\theta}) = \arg\max \mathbf{P}(r,\theta) \quad (6)$$

Because of its inherent geometrical limitation, linear array beamforming is naturally symmetric about the array itself. This inherent mirror symmetry results in the monitored area being limited to, at most, 180°. In fact, a mirrored lobe will appear in the spatial spectrum obtained by Eq. (6) due to the symmetry of cosine function in Eq. (3).

2.2 2D-MUSIC based impact localization method using uniform linear array

The improved linear array is illustrated in Fig. 1. As mentioned above, two PZT sensors are added above and below the reference sensor of the linear array. By comparing the arriving times of the two additional PZT elements, this array design configuration is able to perform full-range 360°image of the monitored area.

(a) In the case of $t_{\mathrm{U}} \neq t_{\mathrm{D}}$

Seen from Fig.2 and Fig.3, when the impact source occurs above the sensors array, the signal induced by impact must arrive earlier at the upper PZT sensors than the lower PZT sensors, that is $t_{\mathrm{U}} < t_{\mathrm{D}}$.

Therefore, we can compare the arrival time of two PZT sensors before scanning the whole structure using Eq. (6), and Eq. (6) could be rewritten as

$$\{\hat{r},\hat{\theta}_1\} = \arg\max \mathbf{P}(r,\theta_1), 0° < \theta_1 < 180°, t_{\mathrm{U}} > t_{\mathrm{D}} \quad (7)$$

And

$$\{\hat{r},\hat{\theta}_1\} = \arg\max \mathbf{P}(r,\theta_1), 180° < \theta_1 < 360°, t_{\mathrm{U}} > t_{\mathrm{D}} \quad (8)$$

(b) In the case of $t_{\mathrm{U}} = t_{\mathrm{D}}$

However, the time of impact signal arrivals at the PZT U will be equal to the arrival time at PZT D when the impact source occurs along the x axis, shown in Fig. 4. In this situation, the direction of impact can be obtained as

$$\begin{cases} \hat{\theta} = 0°, if \quad t_M < t_{-M} \\ \hat{\theta} = 180°, if \quad t_M > t_{-M} \end{cases} \quad (9)$$

A triangle in this figure is composed of the distance r between impact source and PZT 0, the distance r_{D} between impact source and PZT D, the distance d between PZT 0 and PZT D. According to this triangle, r_{D} can be calculated as

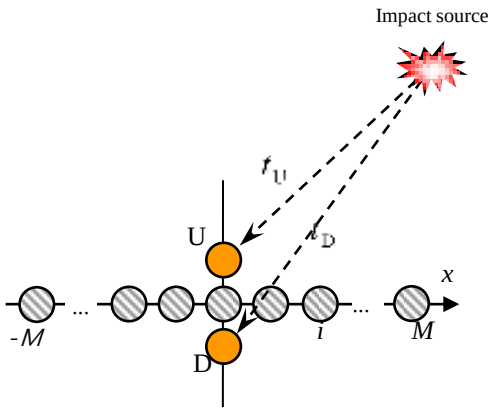

Fig. 2 The time of impact signal arrival at the PZT U and PZT D ($t_{\mathrm{U}} \neq t_{\mathrm{D}}$)

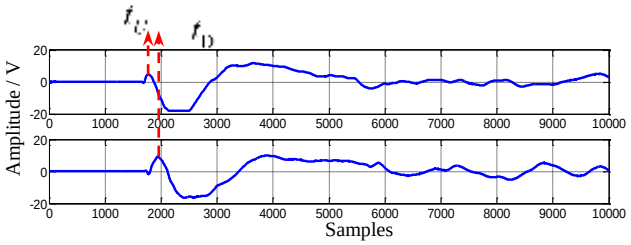

Fig. 3 Impact signals of PZT U and PZT D

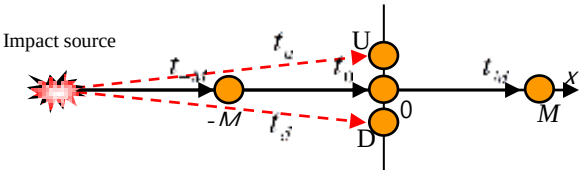

Fig. 4 The time of impact signal arrival at the PZT U and PZT D ($t_u = t_d$)

$$r_{\mathrm{D}} = \sqrt{r^2 + d^2} \tag{10}$$

And

$$r_{\mathrm{D}} - r = c\Delta t_{0\mathrm{D}} \tag{11}$$

Thus, the distance of impact can be obtained as

$$\hat{r} = \frac{d^2 + (c_x \Delta t_{0\mathrm{D}})^2}{c_x \Delta t_{0\mathrm{D}}} \tag{12}$$

where, $\Delta t_{0\mathrm{D}}$ is the time difference between the impact signal arrivals at the PZT 0 and PZT D, and c_x is the velocity of impact signal propagating along the x axis. This velocity can be represented by the time difference Δt_{-MM} between the impact signal arrivals at the PZT -M and PZT M.

$$c_x = \frac{2Md}{\Delta t_{-MM}} \tag{13}$$

And Eq. (12) can be rewritten as

$$\hat{r} = \frac{(\Delta t_{-MM})^2 + 4M^2(\Delta t_{0\mathrm{D}})^2}{2M(\Delta t_{-MM})(\Delta t_{0\mathrm{D}})} d \tag{14}$$

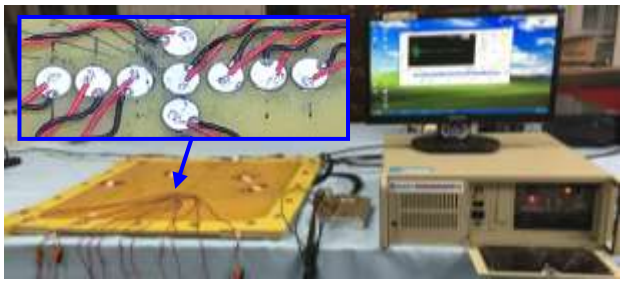

(a) Experimental systems

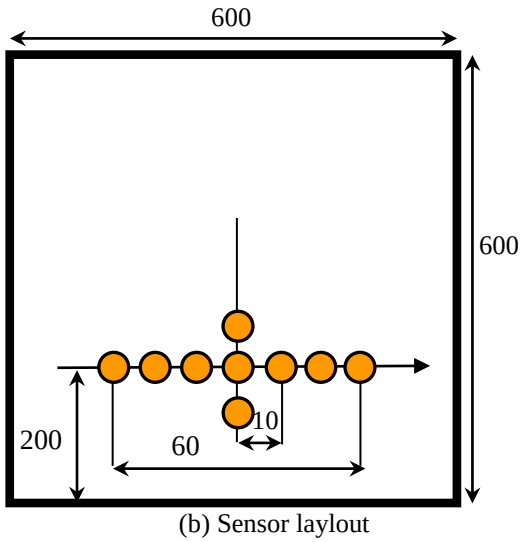

(b) Sensor laylout

Fig. 5 Experimental setup and sensor laylout

3. Experiment investigation on a quasi-isotropic epoxy laminate plate

The experiment setup is shown in Fig. 5, including the integrated structural health monitoring scanning system developed by the authors is adopted as the monitoring system. This system is developed to control the excitation and sensing of the PZT sensor array.

The epoxy laminates plate with a dimension of 600 mm × 600 mm × 2 mm. The thickness of each ply is 0.125 mm and the ply sequence is $[0_2/90_4/0_2]_S$. The array used in the experiment is an improved linear array bonded on the structure surface of opposing panel with 7 PZT sensors (PZT Type: P-41, Manufacture: China HengSheng Acoustics Electron Apparatus Co., Ltd). The diameter of the PZT sensor is 8 mm. These sensors are arranged with a space of 13 mm and are labeled as PZT -3, PZT -2,…, PZT 3 respectively from the left to the right. Besides, two PZT sensors are added above and below the reference sensor, labeled as PZT U and PZT D. The sampling rate is set to be 10 MHz, and set the PZT 0 as the trigger channel, and the trigger voltage is set to 3V in the experiments. The sampling length is 30000 including 6000 pre-trigger samples.

Take the impact at (100 mm, 90°) as an example. Table 1 shows all eigenvalues of the covariance matrix of each impact event. The number of impacts N can be obtained by using a subjective threshold $\lambda_{\mathrm{T}} = 0.1\lambda_1$ [12]. The threshold value of each could be calculated, that is $\lambda_{\mathrm{T}} = 4.8$, and the number of impact events can be estimated by counting the eigenvalues, that is $N = 1$. Fig. 6(a) shows the narrow band signals extracted of PZT U and PZT D at the center-frequency of 50 kHz and their envelopes. The measured phase velocity c of 50 kHz obtained is 1270 m/s. It shows that the impact signal arrives earlier at the PZT U than PZT D. Using the 2D-MUSIC algorithm, the impact occurring direction and distance can be simultaneously found from the spatial spectrum shown in Fig. 6(b), the predicted position of impact at the point (100 mm, 90°) is (100 mm, 91°) whose error of direction estimation is 1° and the error in distance estimation is 0 mm.

Take the impact at (100 mm, 0°) as anther example which lies in x axis. Fig. 7(a) shows that the impact signal arrives at the PZT U and PZT D is almost the same, that is $t_D = t_U$. Therefore, the impact source occurs along the x axis. And the impact signals extracted from each sensor are shown in Fig. 7(b).

From this figure, we can obtain the arrival time of each PZT as follow,

$t_{-3} = 0.5909$ ms, $t_3 = 0.5262$ ms, $t_{\mathrm{U}} = 0.5589$ ms, $t_0 = 0.5571$ ms, $t_{\mathrm{D}} = 0.5582$ ms

Table 1 Eigenvalues distributions of the covariance matrix

Subspace	Signal	Noise					
Eigenvector	λ_1	λ_2	λ_3	λ_4	λ_5	λ_6	λ_7
	48.867	0.371	0.011	0.001	0.0004	0.0003	0.0002

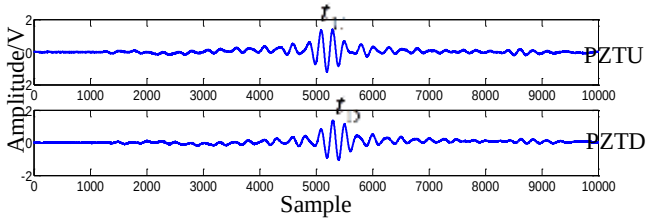

(a) The narrow band extracted of PZT U and PZT D and their envelopes

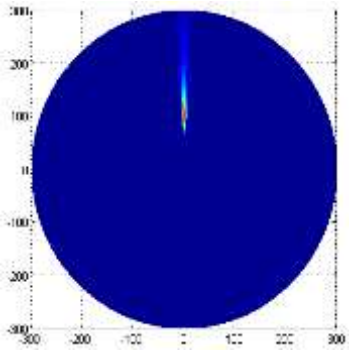

(b) Spatial spectrum

Fig. 6 The estimated result by 2D-MUSIC at impact point (100 mm, 90°)

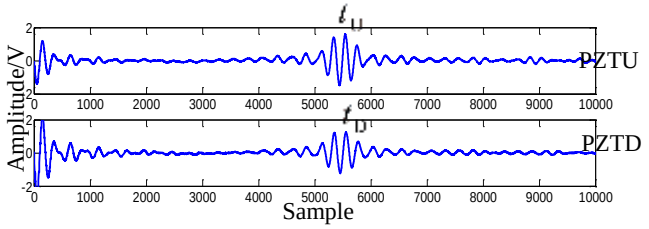

(a) PZT U and PZT D

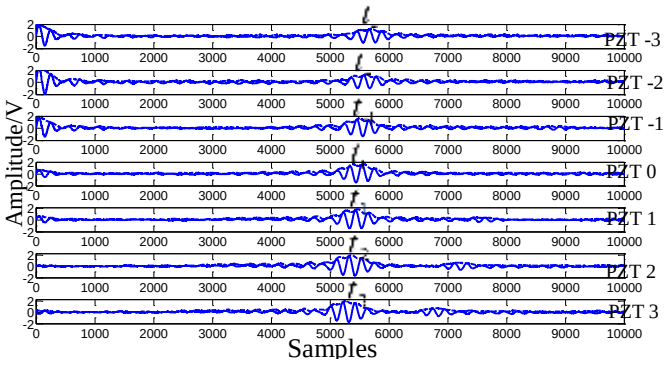

(b) PZT-3 to PZT3

Fig. 7 The narrow band extracted and their envelopes of impact point (100 mm, 0°)

Since $t_{-3} > t_3$, the predicted direction of impact $\theta = 0°$. And the distance of impact can be calculated using Eq. (14) as

$$\Delta t_{-33} = t_{-3} - t_3 = 0.0647 \text{ ms}$$

$$\Delta t_{0D} = t_0 - t_D = 0.0011 \text{ ms}$$

$$\hat{r} = \frac{(\Delta t_{-MM})^2 + 4M^2(\Delta t_{0D})^2}{2M(\Delta t_{-MM})(\Delta t_{0D})} d = 98.03 \text{ mm}$$

Therefore, the predicted position of impact at the point (100 mm, 0°) is (98.03 mm, 0°) whose error of direction estimation is 0° and the error in distance estimation is 1.97 mm. The predicted position of impact at the point (100 mm, 0°) using plum-blossom sensor array in reference [19] is (83 mm, 5°) whose error of direction estimation is 5° and the error in distance estimation is 17 mm. Note that the prediction of the impact along the *x*-axis using this improved linear array are more close to the actual locations of the impact source than that using plum-blossom sensor array.

4. Evaluation on a stiffened composite panel

4.1 Experiment setup

As seen in Figs. 8 and 9, the size of the stiffened composite structure is 1040 mm×1820 mm×4 mm, which is made of carbon fiber composite material. The panels are fastened to the steel box frame. There are in total six T-shaped stiffeners with a distance of 130 mm between them on the panels. Vertical to the stiffeners there are in total five rows of bolt holes. The distance between the lines is 280 mm. Sensor array layout is similar with the experiment investigation on a quasi-isotropic epoxy laminate plate. The sampling rate is set to be 2 MHz, and set the PZT 0 as the trigger channel, and the trigger voltage is set to 3V in the experiments. The sampling length is 20000 including 2000 pre-trigger samples.

4.2 Typical impact response signals

This composite stiffened composite panel contains lots of stiffeners and the distance between them is very short. The stiffeners can reduce the amplitude of signals which are propagating through them, and can cause mode conversion, and may affect the dispersion of each mode (Reynolds *et al.* 2010), shown as Fig. 10, the S0 mode and A0 mode from the impact response signals could be determined by their velocities and amplitudes. And bolt holes on them also can introduce a lot of reflecting signals. To research the stiffeners and bolt holes affect separately, a sub-region is divided between the 2nd and 3rd bolt holes.

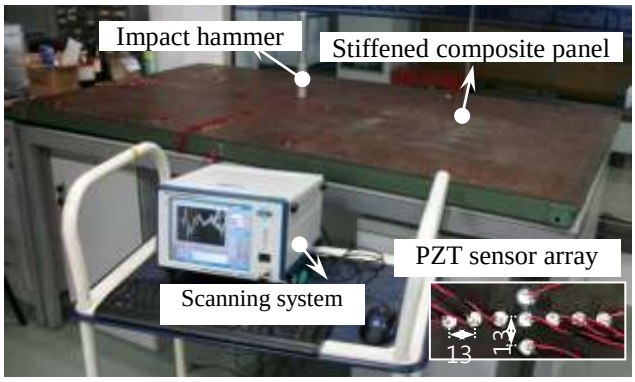

Fig. 8 Experiment setup of impact localization

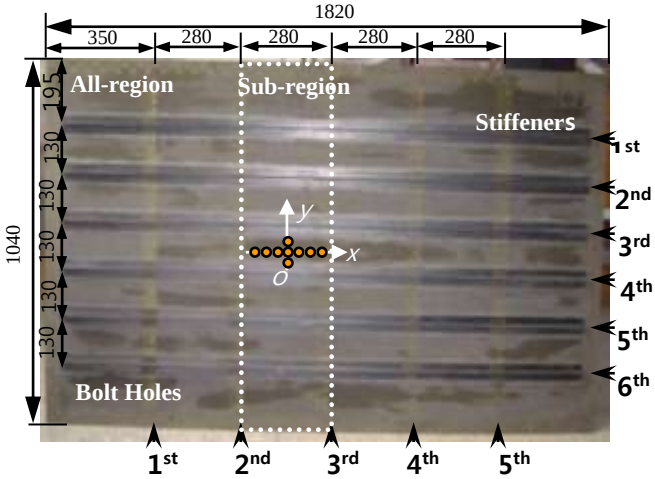

Fig. 9 Stiffened composite panel

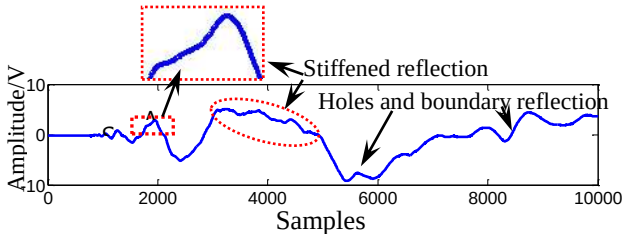

Fig. 10 The original impact signal propagating in the stiffened composite structure

A typical impact at the point (200 mm, 90°) is chosen as a typical case to be analyzed first. When this impact occurs, the output of each PZT sensor in the ULA is shown in Fig. 11. Fig. 12 shows the frequency spectrum of PZT1 which is a typical one representing the frequency characters of the impact induced elastic wave signal obtained by the PZT sensors. From Fig. 12, it can be concluded that the energy of the impact signal is mainly in the frequency band from 0 Hz to 4 kHz.

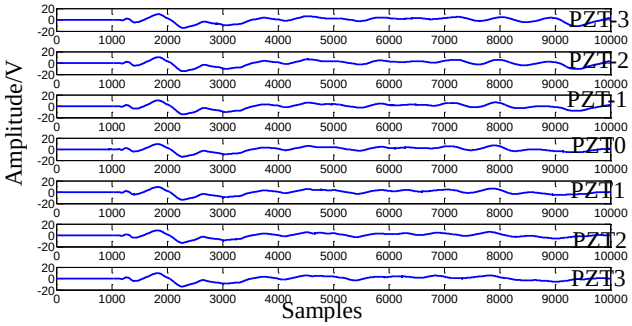

Fig. 11 Typical output of the PZT sensors when impact occurs at (200 mm, 90°)

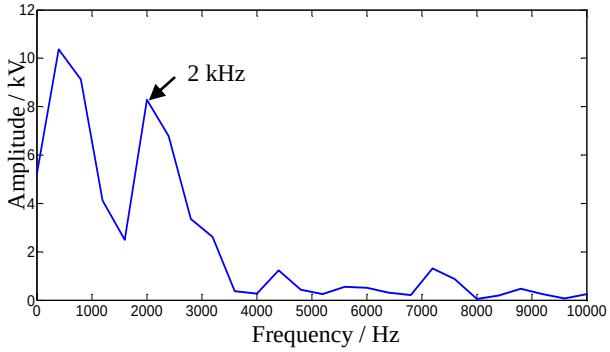

Fig. 12 The frequency spectrum of impact signal obtained by PZT1

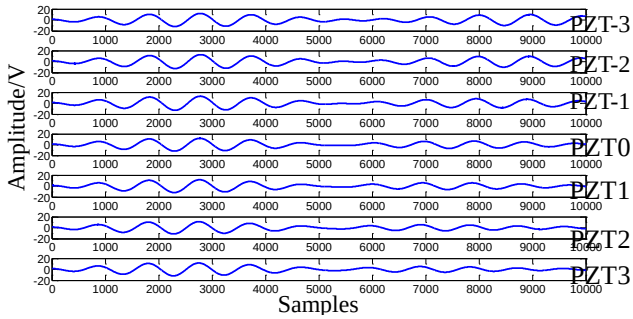

Fig. 13 The narrow band impact signals extracted at the center-frequency of 2 kHz

To guarantee the time resolution and narrow-band signal extraction, 2 kHz is selected as the central frequency in the narrow-band signal extraction processing. The impact signals extracted from each sensor are shown in Fig. 13. From Fig. 13, the wave fronts of the A0 wavefronts of the signals are marked with dashed lines which can be easily found. Besides, the narrow band extracted of PZT U and PZT D at the center-frequency of 2 kHz and their envelopes are shown in Fig. 14, and it shows that the impact signal arrives earlier at the PZT U than PZT D. The measured phase velocity c of 2 kHz obtained is 450 m/s.

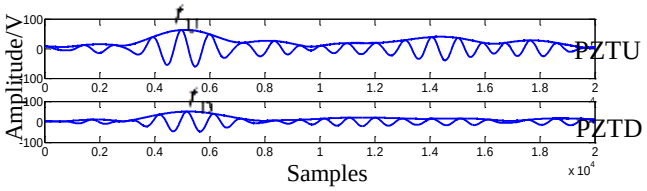

Fig. 14 The narrow band extracted of PZT U and PZTD and their envelopes

4.3 Impact localization results and discussion

4.3.1 Sub-region

The impact extracted signals are used to form the input vector of the 2D-MUSIC model. According to the structure dimension, the scanned area is set to be the distance from 0 to 450 mm and the direction from 0° to 360°, and the scanning step length of the distance and direction is 1 mm and 1° respectively.

A typical spatial spectrum $\mathbf{P}(r,\theta)$ obtained is shown in Fig. 15. The figure represents spatial spectrum magnitudes of each scanned point (r,θ), and the highest pixel point of the figure represents the impact point localized by the presented 2D-MUSIC algorithm. Because of the inherent geometrical limitation of linear array, two highest pixel points appear symmetrically about the x axis, shown as Fig. 15(a). The narrow band extracted of PZT U and PZT D at the center-frequency of 2 kHz and their envelopes, shown in Fig.14, shows that the impact signal arrives earlier at the PZT U than PZT D. Therefore, the impact must occur above the sensors array (x axis), and the improved spatial spectrum $\mathbf{P}(r,\theta)$ can be obtained as Fig. 15(b). The predicted position of impact is (202mm, 87°) whose error of direction estimation is 3° and the error in distance estimation is 2 mm.

According to the section 2.2, there exists the time of impact signal arrival at the PZT U will be equal to the arrival time at PZT D, when the impact source occurs along the x axis. Another typical impact at the point (100 mm, 0°) is chosen as this case to be analyzed. The narrow band extracted of PZT -3, PZT 3, PZT U, PZT 0 and PZT D at the center-frequency of 2 kHz can be obtained using wavelet transform as follow,

$t_{-3}=1.276$ ms, $t_3=0.9785$ ms, $t_U=1.1715$ ms, $t_0=1.1635$ ms, $t_D=1.1715$ ms

Since $t_{-3}>t_3$, the predicted direction of impact $\theta=0°$. And the distance of impact can be calculated using Eq. (14) as

$$\Delta t_{-33}=t_{-3}-t_3=0.298\,\text{ms}$$

$$\Delta t_{0D}=t_0-t_D=0.008\,\text{ms}$$

$$\hat{r}=\frac{(\Delta t_{-MM})^2+4M^2(\Delta t_{0D})^2}{2M(\Delta t_{-MM})(\Delta t_{0D})}d$$

$$=\frac{(0.298)^2+4\times3^2\times(0.008)^2}{2\times3\times(0.298)\times(0.008)}\times13$$

$$=82.8mm$$

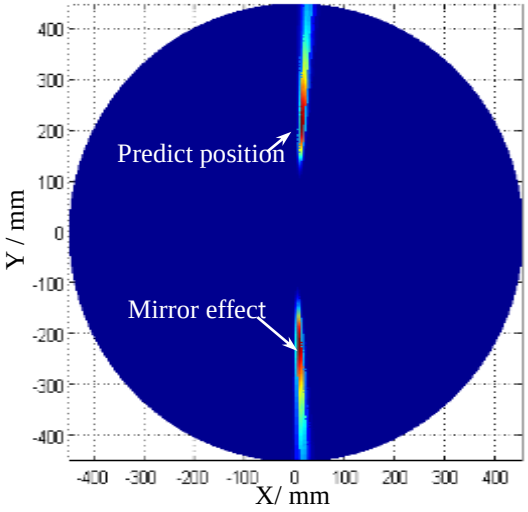

(a) Linear array

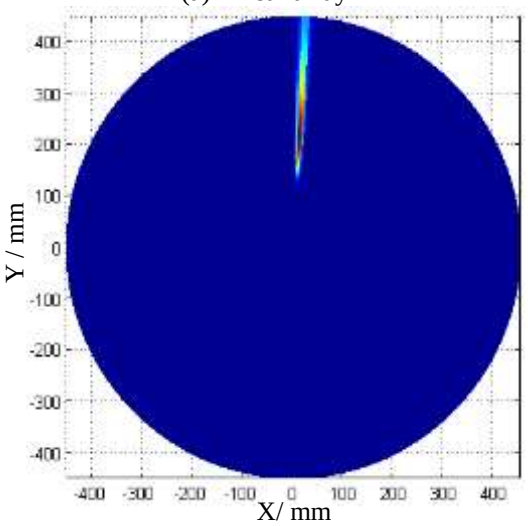

(b) Improved linear array

Fig. 15 The spatial spectrum estimated by 2D-MUSIC at impact point (200 mm, 90°)

Therefore, the predicted position of impact at the point (100 mm, 0°) is (82.8 mm, 0°) whose error of direction estimation is 0° and the maximum error in distance estimation is 18.2 mm.

Fig. 16 gives the results of the predicted impact locations of the fifty impacts on sub-region. The relative errors of impact localization results in sub-region are shown in Fig. 17. The results are in good agreement with the actual location of the applied impact. The maximum error in estimation of the impact location is 37 mm, and most of them are less than 20 mm. All of the relative errors of impact direction and 90% of the relative errors of impact distance are less than 10%.

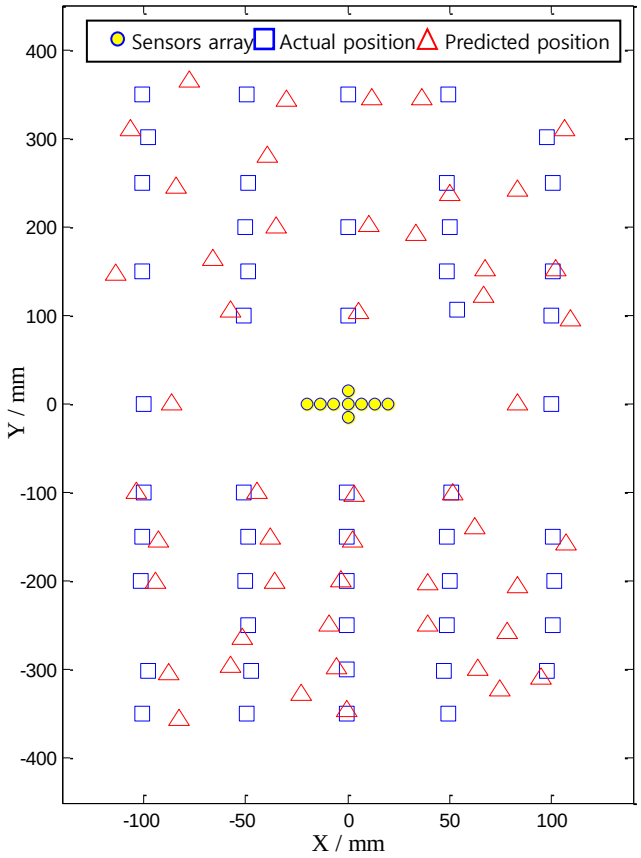

Fig. 16 Impact localization results and comparison in sub-region

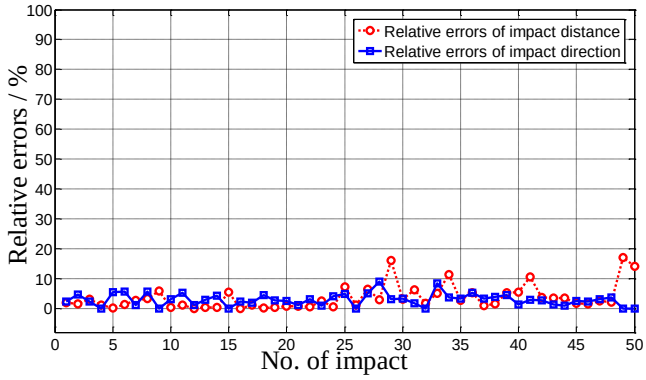

Fig. 17 The relative errors of impact localization results in sub-region

4.3.2 All-region

According to the structure dimension of all-region, the scanned area is set to be the distance from 0 to 1000 mm and the direction from 0^o to 360^o, and the scanning step length of the distance and direction is 1 mm and 1^o respectively. The spatial spectrum $\mathbf{P}(r,\theta)$ of impact at the point (985 mm, 28^o) obtained is shown in Fig. 18. Since the impact signals produced are complex, the predicted position of impact is (909 mm, 28°) whose error of direction estimation is 0^o and the error in distance estimation is 76 mm.

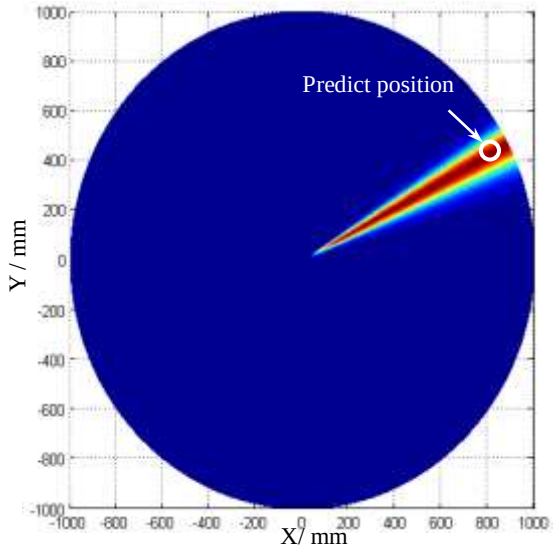

Fig. 18 The spatial spectrum estimated of impact point (985 mm, 28^o)

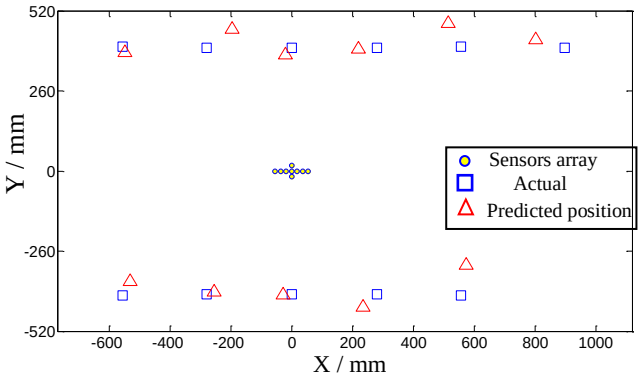

Fig. 19 Impact localization results and comparison in all-region

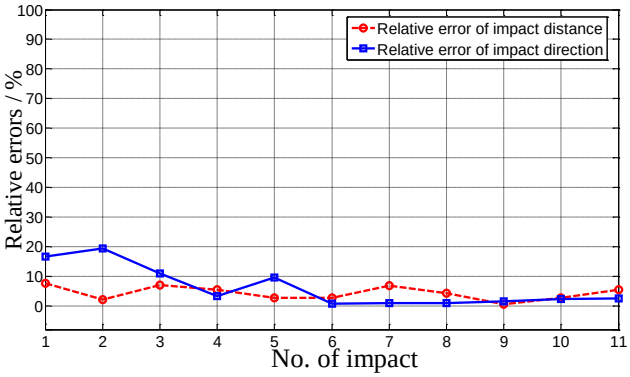

Fig. 20 The relative errors of impact localization results in all-region

Fig. 19 gives the results of the predicted impact locations of the eleven impacts on all-region. The relative errors are shown in Fig. 20, the relative maximum error of impact distance and direction is 19.4% and 7.6%

respectively, but all of distance relative errors and nine of eleven of direction relative errors are below 10%.

5. Conclusions

This paper develops an improved sensor array with two additional sensors above and below the linear sensor array, and presents time difference and two dimensional multiple signal classification (2D-MUSIC) based impact localization for omni-directional localization on composite structures. This array type have fewer elements and is arranged more compact, and is more suitable for complex structures which leave narrow space for array arrangement due to the existing bolt holes, stiffeners, etc. And it can reduce the transmission and reception consistency in other 2-D sensor arrays.

Time difference and 2D-MUSIC based impact localization method using improved linear array is firstly applied on a quasi-isotropic epoxy laminate plate. The impacts at (100 mm, 90^o) and (100 mm, 0^o) are selected as an example to verify the proposed method. Results show that the predictions are very close to the actual locations of the impact source. Then, this proposed method is applied on a complex composite structure which has T-shaped stiffeners and bolt holes. (i) Fifty impacts in sub-region are in good agreement with the actual location of the applied impact. The maximum error in estimation of the impact location is 37mm, and most of them are less than 20mm. All of the relative errors of impact direction and 90% of the relative errors of impact distance are less than 10%. (ii) And eleven impacts along with the structure's boundary in all-region have produced worse results than sub-region. All of distance relative errors and nine of eleven of direction relative errors are below 10%, and the relative maximum error of impact distance and direction is 19.4% and 7.6% respectively.

Further research is still worthy doing to address on the effect of a large complex structure, including stiffeners and bolt holes to improve the accuracy of impact localization in all-region.

Acknowledgments

The research described in this paper was financially supported the National Science Foundation of China (No. 51505339, No.51575400), the Zhejiang Provincial Natural Science Foundation of China (No.LQ16E050005), and Wenzhou university Teaching reform research project (16jg52).

References

Agarwal, K. and Macháň, R. (2016), "Multiple Signal Classification Algorithm For Super-Resolution Fluorescence Microscopy", *Nat. Commun.*, **7**, 13752. https://doi.org/10.1038/ncomms13752.

Cheng, X.Q., Zhao, W.Y., Liu, S.F., Xu, Y.Y. and Bao, JW. (2014), "Damage of scarf-repaired composite laminates subjected to low-velocity impacts", *Steel Compos. Struct.*, **17**(2), 199-213. https://doi.org/10.12989/scs.2014.17.2.199.

Chang, C.M., Chou, J.Y., Tan, P. and Wang, L. (2017), "A sensor fault detection strategy for structural health monitoring systems", *Smart Struct. Syst.*, **20**(1): 43-52. https://doi.org/10.12989/sss.2017.20.1.043.

Chen, X. (2010), "Multiple signal classification method for detecting point-like scatterers embedded in an inhomogeneous background medium", *J. Acoust. Soc. Am.*, **127**(4), 2392. https://doi.org/10.1121/1.3303984.

Engholm, M. and Stepinski, T. (2011), "Direction of arrival estimation of Lamb waves using circular arrays", *Struct. Health Monit.*, **10**(5), 467-480. https://doi.org/10.1177/1475921710379512

Giurgiutiu, V. (2014), Structural Health Monitoring with Piezoelectric Wafer Active Sensors (2nd Ed.), Elsevier, Waltham, MA, USA.

Jeong, H. (2001), "Analysis of plate wave propagation in anisotropic laminates using a wavelet transform", *NDT & E Int.*, **34**(3), 185-190. https://doi.org/10.1016/s0963-8695(00)00056-6.

Mahzan, S.,. Staszewski, W.J. and Worden, K. (2010), "Experimental studies on impact damage location in composite aerospace structures using genetic algorithms and neural networks", *Smart Struct. Syst.*, **6**(2), 838-844. https://doi.org/10.12989/sss.2010.6.2.147.

Moon, Y.S., Lee, S.K., Shin, K. and Lee, Y.S. (2011), "Identification of multiple impacts on a plate using the time-frequency analysis and the kalman filter", *J. Intel. Mat. Syst. Str.*, **22**(12), 1283-1291. https://doi.org/10.1177/1045389X11411216.

Purekar, S., Pines, D., Sundararaman, S. and Adams, D. (2004). "Directional piezoelectric phased array filters for detecting damage in isotropic plates", *Smart. Mater. Struct*., **13**(4), 838-850. https://doi.org/10.1088/0964-1726/13/4/022.

Purekar, A. and Pines, D. (2010), "Damage detection in thin composite laminates using piezoelectric phased sensor arrays and guided lamb wave interrogation", *J. Intel. Mat. Syst. Str.*, **21**(10), 995-1010. https://doi.org/10.1177/1045389X10372003.

Qiu, L., Yuan, S., Zhang, X. and Wang, Y. (2011), "A time reversal focusing based impact imaging method and its evaluation on complex composite structures", *Smart. Mater. Struct.*, **20**(10), 105014. https://doi.org/10.1088/0964-1726/20/10/105014.

Qiu, L. and Yuan, S. (2009), "On development of a multi-channel PZT array scanning system and its evaluating application on UAV wing box", *Sensor. Actuat. A-Phys.*, **151**(2), 220-230. https://doi.org/10.1016/j.sna.2009.02.032.

Ren, Y., Qiu, L., Yuan, S. and Su, Z. (2017), "A diagnostic imaging approach for online characterization of multi-impact in aircraft composite structures based on a scanning spatial-wavenumber filter of guided wave". *Mech. Syst. Signal Pr.*, **90**: 44-63. https://doi.org/10.1016/j.ymssp.2016.12.005.

Reynolds, W., Doyle, D., Brown, J. and Arritt, B. (2010), "Wave Propagation in Rib-Stiffened Structures: Modeling and Experiments", *Proceedings of the ASME 2010 Conference on Smart Materials, Adaptive Structures and Intelligent Systems*, Philadelphia, October.

Wang, Y., Yuan, S. and Qiu, L. (2011), "Improved wavelet-based spatial filter of damage imaging method on composite structures", *Chinese J. Aeronaut.* **24**(5), 665-672. https://doi.org/10.1016/S1000-9361(11)60078-2.

Wang, Z., Yuan, S., Qiu, L. and Liu, B. (2015), "Omni-directional damage detection and localization with a cruciform piezoelectric ultrasonic phased array", *J. Vibroeng.*, **17**(5), 2338-2349.

Yang, H., Lee, Y. and Lee, S. (2013), "Impact source localization in plate utilizing multiple signal classification", *P I Mech. Eng.*,

C-J MES., **227**(C4), 703-713. https://doi.org/10.1177/0954406212452233

Yuan, S., Lai, X., Zhao, X., Xu, X. and Zhang, L. (2005), „Distributed structural health monitoring system based on smart wireless sensor and multi-agent technology“, *Smart. Mater. Struct*,, **15**(1), 1-8. https://doi.org/10.1088/0964-1726/15/1/029.

Yuan, S., Zhong, Y., Qiu, L. and Wang, Z. (2014), "Two-dimensional near-field multiple signal classification algorithm–based impact localization", *J. Intel. Mat. Syst. Str.*, **26**(4), 400-413. https://doi.org/10.1177/1045389X14529026.

Yang, H., Shin, T.J. and Lee, S.K. (2014), "Source location in plates based on the multiple sensors array method and wavelet analysis", *J. Mech. Sci. Techenol.*, **28**(1), 1-8. https://doi.org/10.1007/s12206-013-0938-5.

Yuan, S., Bao, Q., Qiu, L. and Zhong, Y. (2015),"A single frequency component-based re-estimated MUSIC algorithm for impact localization on complex composite structures", *Smart. Mater. Struct.*, **24**(10), 105021. https://doi.org/10.1088/0964-1726/24/10/105021.

Zhong, Y., Yuan, S. and Qiu, L. (2014), "Multi-impact source localisation on aircraft composite structure using uniform linear PZT sensors array", *Struct. Infrastruct. E.*, **11**(3), 310-320. https://doi.org/10.1080/15732479.2013.878732.

Zhong, Y. and Xiang, J. (2016), "A two-dimensional plum-blossom sensor array-based multiple signal classification method for impact localization in composite structures". *Comput.-Aided Civ. Inf.*, **31**(8), 633-643. https://doi.org/10.1111/mice.12198.

CC